Population of superdeformed excitations in ^{198}Po

M. S. Johnson,[1,*] J. A. Cizewski,[1] M. B. Smith,[1,†] J. S. Thomas,[1] J. A. Becker,[2] L. A. Bernstein,[2] A. Schiller,[2,‡] D. P. McNabb,[2] P. Fallon,[3] and A. O. Macchiavelli[3]

[1]*Department of Physics and Astronomy, Rutgers University, New Brunswick, NJ 08903*

[2]*Lawrence Livermore National Laboratory, Livermore, CA 94550*

[3]*Lawrence Berkeley National Laboratory, Berkeley, CA 94720*

(Received 26 May 2004; published 28 February 2005)

Superdeformed excitations in ^{198}Po were studied using the ^{174}Yb(^{29}Si,5n) reaction and γ-ray spectroscopy with Gammasphere. Energy-spin entry distributions for populating normal (ND) and superdeformed (SD) excitations were extracted by gating on discrete ND and SD transitions, respectively. Information on the SD excitation energy, SD well depth, and fission barrier in ^{198}Po was deduced.

DOI: 10.1103/PhysRevC.71.024317 PACS number(s): 21.10.Re, 23.20.Lv, 25.70.Gh, 27.80.+w

I. INTRODUCTION

It is important for the study of the structure of atomic nuclei to understand the limits of nuclear existence as functions of neutron and proton number, as well as excitation energy, angular momentum, and elongation. The role that microscopic shell corrections play in enhancing and in extending the limits of nuclear stability is central to this understanding. The present work studies highly elongated, superdeformed (SD) excitations near the limits of instability to fission to probe the macroscopic nuclear surface energy potential in the presence of large-scale microscopic shell corrections. Understanding this micro-macro interplay requires measurements of the energy and spin of SD excitations, the population mechanisms of highly elongated structures, and the decay modes to excitations with "normal" (ND) deformations.

The present work focuses on ^{198}Po, the most fissile nucleus in which an SD rotational band has been observed at high spin [1]. McNabb and coworkers [1], using Gammasphere Phase I with 56 detectors, observed the rotational band associated with SD in ^{198}Po, predicted by [2,3]. Because fission preferentially carries off the higher angular momentum partial waves in fusion reactions, the population of both ND and SD excitations at relatively high spins is limited. In addition, for each evaporated neutron, the residue becomes more fissile, because the Z^2/A ratio, a measure of fissility, increases. McNabb *et al*. determined that the highest spin state populated in SD ^{198}Po is 26$\hbar$; measurements of ND states [4,5] show that 22$\hbar$ is the highest ND spin populated.

The best method to determine the energy and spin of SD excitations is to measure directly the one-step transitions that connect specific SD and ND states [6–10]. Using the known excitation energy, spin, and parity of the final ND state, the quantum numbers of the initial SD level can be deduced. However, these single-step γ-ray transitions are a small part of the intensity of the SD decay spectrum, and their intensity is further suppressed for SD states with high excitation energy. Observing such one-step transitions is further complicated in SD bands that are weakly populated, when the fusion cross sections are small and when there are many open channels, in particular fission, that limit the population of a specific SD cascade.

Another approach has been adopted in the present work: a measurement of the entry distribution in energy and spin that populates SD excitations. As described, such measurements can be used not only to estimate the energy of SD excitations but also to provide information on the barrier that separates the ND and SD minima in the potential energy surface and the limits of energy and angular momentum populated in a system with competition from fission.

II. EXPERIMENTAL SETUP

The experiment was performed at the 88-inch Cyclotron Facility at the Lawrence Berkeley National Laboratory. γ-ray spectroscopy measurements were made using the Gammasphere array with 101 Ge detectors and without hevimet collimators. High-spin states in ^{198}Po were populated using the ^{174}Yb(^{29}Si,5n) reaction with a beam energy of 148 MeV. Ta-Cu absorbers were placed in front of the Ge detectors and thick Pb absorbers replaced the hevimet collimators in front of the BGO scintillators to reduce the intensity of x rays. Two separate ^{174}Yb targets of areal density 1.08 and 0.91 mg/cm^2 evaporated onto approximately 8.7 mg/cm^2 Au backings were used. A total of 1.9×10^9 fourfold events were collected for analysis.

III. RESULTS FOR POPULATION OF ^{198}Po

The intensities of the transitions associated with SD ^{198}Po are listed in Table I. The information was extracted from summed double-gate combinations using the same gate combinations used in Ref. [1] and energy-dependent time gates. Background subtraction was implemented using the FUL algorithm [11], and the intensities were corrected for

*Present address: Oak Ridge Associated Universities, Oak Ridge, TN 37831.

†Present address: TRIUMF Vancouver, B.C. Canada V6T 2A3.

‡Present address: NSCL Michigan State University, East Lansing, MI 48824.

TABLE I. Energies, spins, and relative intensities of ^{198}Po SD transitions.

Spin ($\hbar$)[a]	Energy (keV)	Intensity[b]
8	175.90(13)	$\lesssim$9
10	220.43(14)	0.47(3)
12	264.37(13)	0.81(2)
14	307.41(16)	0.93(3)
16	349.52(13)	$\equiv$1.00(8)
18	390.58(19)	0.89(8)
20	429.77(21)	0.84(7)
22	467.9(3)	0.80(6)
24	505.9(7)	0.44(8)

[a]Spins deduced by McNabb [1].
[b]Intensities have been corrected for detector efficiency and electron conversion.

electron conversion. The results in Table I are in agreement with those in Ref. [1].

Entry distributions in energy and angular momentum (E,I) were deduced from measured distributions (H,K) in the Gammasphere array of the total sum energy, H, and the number of detectors that fired, K, for each event. The challenge was to extract (H,K) matrices associated with SD in ^{198}Po, with minimal contamination from the dominant fission channel. It was not possible to extract (H,K) matrices double gated on SD transitions, because all standard background subtraction techniques oversubtracted the (H,K) matrices at the maximum in the distribution. Therefore, threefold SD gates were used to generate (H, K, E_γ) matrices, because threefold coincidences enhanced real SD excitations while minimizing contributions from background. Clean sets of γ-γ-γ gates were chosen from the same gates used in Ref. [1] to extract the (H,K) matrices associated with ^{198}Po SD. Energy-dependent time gates were used for both the high-resolution discrete γ-ray spectra and (H,K) matrices. To extract results for low statistics data, the (H,K) matrix was binned to 1 MeV for H and one unit of K. The projection of the (H, K, E_γ) matrix on the E_γ axis is displayed in Fig. 1. It is important to note that this spectrum is not background subtracted, which implies that the associated (H,K) matrix is also not background subtracted. The intensities in Fig. 1 are in agreement with those listed in Table I.

To ensure that the elements of the matrix are associated with the SD structure in ^{198}Po, each pixel in the (H,K) matrix was normalized by its associated high-resolution E_γ spectrum. To determine the SD band contribution in each (H,K) pixel, the counts were normalized to the counts of a transition in coincidence with the SD band. This method effectively fourfold gates the data set and subtracts background. Because of the low SD-band statistics in spectra that require 3 SD transitions in coincidence, the 605-keV $2^+ \longrightarrow 0^+$ transition in ^{198}Po was used to normalize each (H,K) pixel. Therefore, the extracted (H,K) distribution is associated with SD transitions and their decay to low-lying ND states that bypasses the ND isomers [12] at $\sim 10\hbar$.

The (H,K) matrix was then unfolded according to the method discussed in Ref. [13] using the measured [14]

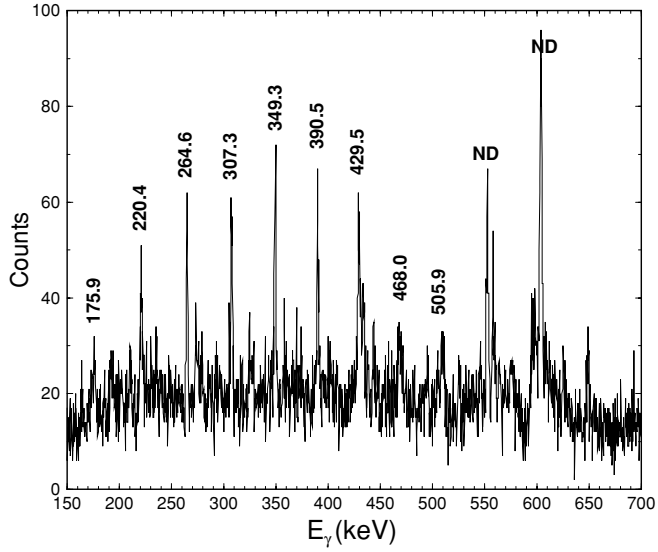

FIG. 1. Spectrum of ^{198}Po SD band threefold gated on SD band transitions.

response of the Gammasphere array to convert (H,K) to (E_{ex}, M_γ), where E_{ex} is the excitation energy and M_γ is γ-ray multiplicity. The unfolding procedure was allowed to go through 10 iterations. The measured response [14] was determined for a setup similar to the present experiment, with no Hevimet collimators; we assumed that the time gates on the BGO detectors were the same. Uncertanties associated with the differences between the response measurement and the experiment are unknown, but assumed small based on the similarities of the setups.

Finally, realistic model assumptions were used to convert (E_{ex}, M_γ) to (E_{ex}, I) [13] as follows:

$$I = \Delta I(M_\gamma + N_{e^-} - N_{\text{stats}}) + \Delta I_{\text{stats}} N_{\text{stats}}, \quad (1)$$

where ΔI is the average spin carried by each γ ray, N_{e^-} is the number of conversion electrons per cascade, N_{stats} is the average number of statistical γ rays emitted per cascade, and ΔI_{stats} is the average spin carried off by each statistical transition. The values are summarized in Table II. ΔI is deduced from the measured average spin carried by the respective ND or SD cascade. The number of conversion electrons, N_{e^-}, was deduced from the conversion coefficients for the transitions involved in the respective ND or SD cascade. N_{stats} and ΔI_{stats} were assumed from model calculations for ^{192}Hg [13,15], which were shown to be valid for other isotopes in the $A \sim 190$ region for quasicontinuous SD decay studies such as ^{192,194}Pb [16] and ^{195}Pb [17,18]. No correction

TABLE II. Estimates for quantities in Eq. (1) based on realistic assumptions and the model calculations reported in [13].

Assumption	SD	ND
ΔI	1.9	1.7
N_{e^-}	1.66	4.50
N_{stats}	3.0	5.0
ΔI_{stats}	0.5	0.5

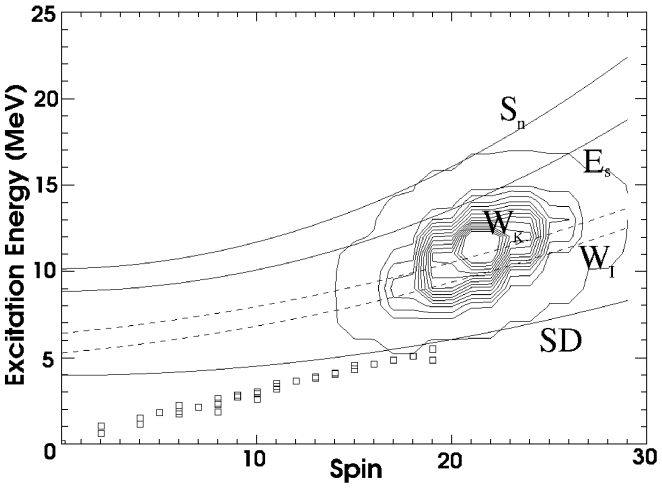

FIG. 2. Entry distribution contours of SD excitations in ^{198}Po. The squares are ND states in ^{198}Po. Lines are used to delineate the Krieger SD yrast line, SD, the well depth, W_I, the Krieger well depth, W_K, and the neutron separation energy, S_n as a function of spin, and the saddle energy E_s. The contours begin at the lowest count and increase by 100 counts for each of the 15 contours. See text for more details.

for possible BGO signals below the threshold was included because such a correction would be less than the uncertainties in H and K. Deduced values of $\Delta I \sim 2$ in Table II are consistent with assumptions made for other nuclei [19,20] in which similar analyses were conducted.

The (E,I) entry distribution associated with the SD yrast band in ^{198}Po is displayed in Fig. 2. Superimposed on this figure is the measured SD yrast line, extrapolated to zero spin using the moment of inertia obtained from the average spacing of the observed SD band γ-ray energies [1,17]. The excitation energy of 3.95 MeV at zero spin was taken from Krieger and coworkers [2].

It is important to note that the threefold gating technique used in this analysis biases the distribution in Fig. 2 to a region $\geqslant 6\hbar$. We feel that this bias does not affect the present analysis because the centroids of the distributions in Figs. 2 and 4 occur at spins greater than $6\hbar$.

IV. DISCUSSION

Fusion-evaporation reactions populate a nucleus in a region of energy-spin phase space (E,I), the entry distribution. Although the breadth and width of this distribution depends on the spread in energy of the evaporated neutrons and by the impact parameters of the specific reaction, the distribution is fundamentally limited by the neutron separation energy, S_n, the fission barrier, and the yrast line of the specific residue. In ^{198}Po the value of S_n is 10 MeV [22], larger than the predicted [21] fission barrier of 8.83 MeV at zero spin. Therefore, fission, rather than neutron separation energy, is expected to restrict the energy-spin phase space in ^{198}Po.

These expected limits of the (E,I) entry distribution for ^{198}Po SD are illustrated in Fig. 2. The lower limit is the measured SD yrast line, using the predicted excitation energy of 3.95 MeV from Ref. [2]. The minimum of the SD entry distribution can provide a realistic estimate of the actual SD yrast line, because it is expected that SD excitations are populated "cold," that is, with relatively low excitation energy above the yrast line. (This is not expected for ND excitations, because these states are populated "hot" with a marked separation between the ND yrast line and the entry distribution.)

The expected upper limit is the saddle energy, E_s, deduced from Sierk fission barriers [21] and the slope of the ND yrast line. Also superimposed is the neutron separation energy, S_n, again with the spin dependence of the ND yrast line. Because the excitations in the ND well are single particle in character, the functional form of the yrast line was determined by a fit of the known [4,5] ND excitations to a quantum rotor. Again, the observed entry distribution has an upper bound restricted by E_s, with a small fraction of the population extending toward the neutron separation energy.

One goal of the present study was to extract the excitation energy of the SD band in ^{198}Po. The lower limits of the (E,I) entry distribution in Fig. 2 of SD ^{198}Po are consistent with the SD excitation energy of 3.95 MeV predicted by Ref. [2]. This is also illustrated in Fig. 3. The lower limits of the entry distribution, displayed as the centroids of the lowest extent of the energy tail ($\sim 3\sigma$) at a given spin of the energy-spin distribution. The uncertainties shown in Fig. 3 were calculated from the statistical uncertainties of these centroids. The lower limits of the measured (E,I) entry distribution for SD ^{198}Po were fit to the expression:

$$E_x = E_{\mathrm{SD}} + 0.006I(I+1), \tag{2}$$

where E_{SD} is 3.9(4) MeV with a $\chi^2_\nu = 1.03$. The coefficient for the spin-dependent rotor term in Eq. (2) was determined by the SD moment of inertia deduced from the measured transitions. The uncertainty in E_{SD} is a conservative estimate from assuming that no data point in Fig. 3 should lie above the SD yrast line because of the definition of yrast and no point should lie below the range of the SD yrast because of our assumption that SD states are fed cold.

The present results can also be used to extract information on the depth of the SD minimum or, analogously, the height of the inner barrier between the SD and ND wells. Because current models [23] of the population of SD excitations suggest that SD states are fed within 1 or 2 MeV of the inner barrier,

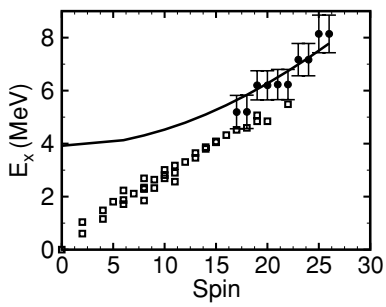

FIG. 3. Lower limits (filled circles) of the entry distribution for SD ^{198}Po compared to the SD yrast line (solid line) with SD bandhead energy of 3.9 MeV. The ND levels are indicated by the open squares.

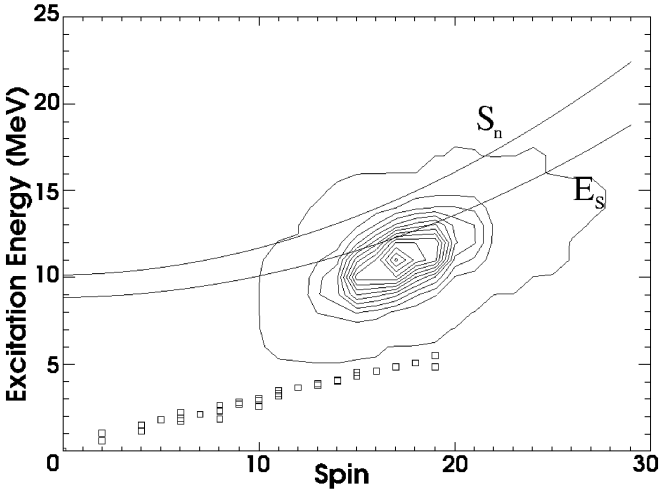

FIG. 4. Entry distribution contours of ND excitations in ^{198}Po. The squares are ND states in ^{198}Po taken from [4,5]. The E_s line is the saddle energy [21] as a function of spin. See caption for Fig. 2.

the centroid of the entry distribution can be used as a measure of the well depth. Given the centroid of the (E,I) distribution of 11 MeV at 21$\hbar$, or 4.8 MeV above the SD yrast line, the well depth is about 3.3(5) MeV at this spin. Krieger and coworkers [2] have predicted a well depth of 2.5 MeV for the SD well at zero spin and it is expected that the SD minimum is more robust at higher spin. A well depth of 2.0(3) MeV at 10$\hbar$ with a modest spin dependence of 6.5% per unit of $\hbar$ has been deduced from preliminary studies [17] of the discrete ^{198}Po SD transitions, using methods outlined in Krücken [24]. Superimposed on Fig. 2 then is the expected depth, W_K, of the ^{198}Po SD well predicted by Krieger [2] and the depth W_I, deduced from the analysis of the discrete transitions [1,17], where the spin dependence from the preliminary analysis of the discrete transitions has been adopted. Both the Krieger [2] and empirical [17] well depths are consistent with the observed centroid of the entry distribution.

To probe further the feeding of the SD excitations in ^{198}Po, the projections in energy and spin of the SD (E,I) entry distribution are displayed in Fig. 5 and compared to the projections of the (E,I) entry distribution gated on ND excitations in ^{198}Po in Fig. 4. As expected, both the energy and spin projections of the SD entry distribution are a subset of the ND entry distributions. The SD excitations in ^{198}Po are populated at higher average spin than ND excitations, as expected for SD excitations that are populated closer to the yrast line or at higher spin for similar excitation energy.

Table III summarizes the centroids for the energy and spin projections of the entry distributions for ND and SD excitations in ^{198}Po. These are compared to the results [13] for the entry distributions associated with ND and SD excitations in ^{192}Hg. Although the energy projections for ND and SD excitations in ^{198}Po are similar, there is a marked difference between the SD and ND energy projections in ^{192}Hg, where the SD excitations are preferentially populated at higher energy.

Of more interest is the maximum spins of the entry distribution. The population of the SD band in ^{198}Po extends to 30$\hbar$, which is only a few units of spin higher than the highest

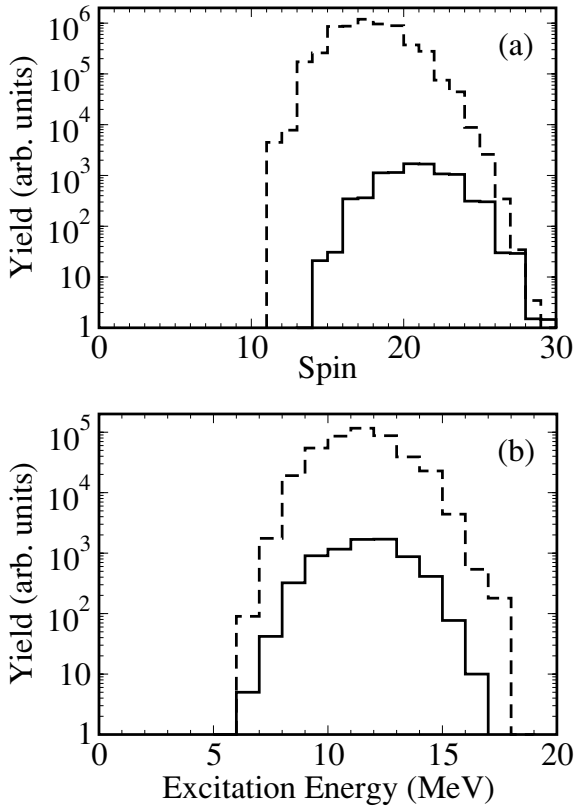

FIG. 5. (a) Spin projections of the entry distributions for SD (solid line) and ND (dashed line) excitations in ^{198}Po. (b) Energy projections of the entry distributions for SD (solid line) and ND (dashed line) excitations in ^{198}Po.

observed [1] discrete SD transition 26 $\longrightarrow$ 24 and considerably less than the 40$\hbar$ (at midtarget) predicted [25] for the fusion reaction ^{29}Si + ^{174}Yb with a beam energy of 148 MeV. The feeding of the ND excitations also extends to 28$\hbar$, which is a few units higher than the highest observed discrete transition 22 $\longrightarrow$ 20 in ^{198}Po placed by McNabb [5]. This limit in the angular momentum available to populate SD and ND excitations in ^{198}Po is in contrast to earlier results [13] for ^{192}Hg, where the population of SD excitations was observed to extend to 50$\hbar$. The present results support the interpretation that fission of the compound nucleus preferentially removes the high angular momentum partial waves of the heavy-ion reaction that populates ^{198}Po.

TABLE III. Centroids of (E,I) entry distributions for SD and ND excitations in ^{198}Po and ^{192}Hg, taken from the present work and [13].

Spectrum	$\bar{E}_{ex}$ (MeV)	$I(\hbar)$
^{198}Po ND	11.0(5)	17.3(4)
^{198}Po SD	11.1(7)	21.4(5)
^{192}Hg ND	∼17	∼32
^{192}Hg SD	∼18	∼36

V. CONCLUSIONS

To summarize, the entry distributions in energy and spin associated with superdeformed excitations in ^{198}Po have been extracted. The lower limit of this distribution was used to estimate the SD excitation at $21\hbar$ of 6.2(5) MeV, which extrapolates to 3.9 MeV at zero spin. The maximum of the entry distribution (at 11.1 MeV, $21\hbar$) is 4.8 MeV above the SD yrast line. Assuming that SD excitations are populated within 1 or 2 MeV of the SD barrier height, an SD well depth of $\sim$3.3(5) MeV at $11\hbar$ can be deduced.

The present results are in good agreement with the work of Krieger and coworkers [2] where an SD excitation energy of 3.95 MeV and well depth of 2.46 MeV at zero spin were predicted. Preliminary analysis [17] of the discrete transitions in ^{198}Po suggests that the depth of the SD well is 2 MeV at $10\hbar$ with a modest spin dependence. Adopting this spin dependence, the ^{198}Po SD well depth at $21\hbar$ deduced from the entry distribution is consistent with both the predictions of Ref. [2] and the preliminary analysis of the ^{198}Po discrete SD transitions.

The study of the total energy and angular momentum populated in the present study of ^{198}Po also supports the expectation that the (E,I) entry distribution should be limited by fission. The upper limit in energy of the measured distribution is consistent with the saddle energy obtained with Sierk fission barriers [21]. The maximum spins populated in both SD and ND entry distributions are considerably less than the expected angular momentum for the ^{29}Si + ^{174}Yb reaction at 148 MeV or the maximum spins observed in ^{192}Hg.

The present analysis of ^{198}Po was challenging because of the low cross section for this evaporation channel coupled with the high γ-ray background, both because of the large fission cross section. Therefore, future studies of such fissile systems would benefit from requiring coincidence measurements between γ rays and evaporation residues, enabling direct gating on transitions associated only with residues and minimizing contributions from other channels, in particular fission.

ACKNOWLEDGMENTS

This work has been supported in part by the National Foundation and U.S. Department of Energy under contract numbers W-7405-ENG-48 (LLNL) and AC03-76SF00098 (LBNL). We also thank Micromatter for providing the gold-backed targets.

[1] D. P. McNabb *et al*., Phys. Rev. C **53**, R541 (1996).
[2] S. J. Krieger *et al*., Nucl. Phys. **A542**, 43 (1992).
[3] W. Satula *et al*., Nucl. Phys. **529**, 289 (1991).
[4] L. A. Bernstein, Ph.D. thesis, Rutgers University (1994).
[5] D. P. McNabb (1997) (unpublished).
[6] K. Hauschild *et al*., Phys. Rev. C **55**, 2819 (1997).
[7] T. L. Khoo *et al*., Phys. Rev. Lett. **76**, 1583 (1996).
[8] S. Siem *et al*., Phys. Rev. C **70**, 014303 (2004).
[9] A. N. Wilson *et al*., Phys. Rev. Lett. **90**, 142501 (2003).
[10] D. P. McNabb *et al*., Phys. Rev. C **61**, 2474 (1997).
[11] B. Crowell *et al*., Nucl. Instrum. Methods Phys. Res. A **355**, 575 (1995).
[12] A. Maj *et al*., Nucl. Phys. **A509**, 413 (1990).
[13] T. Lauritsen *et al*., Phys. Rev. Lett. **69**, 2479 (1992).
[14] R. V. F. Janssens *et al*., $\sim$Gammasphere experiment: GSFMA 72 (1999).
[15] T. Lauritsen *et al*., Phys. Rev. C **62**, 044316 (2000).
[16] D. P. McNabb *et al*., Phys. Rev. C **61**, 031304 (2000).
[17] M. S. Johnson, Ph.D. thesis, Rutgers University (2003).
[18] M. S. Johnson *et al*. (2005) (submitted to Phys. Rev. C).
[19] M. B. Smith *et al*., Phys. Lett. **B551**, 262 (2003).
[20] P. Reiter *et al*., Phys. Rev. Lett. **84**, 3542 (2000).
[21] A. J. Sierk, Phys. Rev. C **33**, 2039 (1986).
[22] M. Bhat, *Evaluated Nuclear Structure Data File*, Springer-Verlag, Berlin, Germany, (1992), data extracted using online data service from ENSDF database, revised October 2003.
[23] T. L. Khoo *et al*., Nucl. Phys. **A557**, 83c (1993).
[24] R. Krücken *et al*., Phys. Rev. C **54**, 1182 (1996).
[25] J. R. Beene and N. G. Nicolis, Computer code EVAPOR (unpublished); developed from PACE by A. Gavron, Phys. Rev. C **21**, 230 (1980).